

AR-010-266

**O  
T  
S  
D**

Resonance Testing of the Gnome  
Combustor Liner

James Dunlop

DSTO-TN-0093

APPROVED FOR PUBLIC RELEASE

© Commonwealth of Australia

# Resonance Testing of the Gnome Combustor Liner

*James Dunlop*

**Airframes and Engines Division  
Aeronautical and Maritime Research Laboratory**

DSTO-TN-0093

## **ABSTRACT**

This report details the results of a series of experimental tests conducted on a combustor liner of the Rolls-Royce Gnome engine. These tests were undertaken as part of an investigation into the cause of cracking of the combustor liner's splitter vane. A modal analysis of the splitter vane was undertaken and mode shape results are presented over a wide range of natural frequencies. A comparison of strains generated by these modes in the areas of cracking shows that two modes in particular are a possible cause of the cracking. The effects on the splitter vane, of an interference fit between it and the engine rear frame splitter ring, are also quantified both statically and dynamically.

19980706 156

## **RELEASE LIMITATION**

*Approved for public release*

DEPARTMENT OF DEFENCE

DEFENCE SCIENCE AND TECHNOLOGY ORGANISATION

*Published by*

*DSTO Aeronautical and Maritime Research Laboratory  
PO Box 4331  
Melbourne Victoria 3001*

*Telephone: (03) 9626 7000*

*Fax: (03) 9626 7999*

*© Commonwealth of Australia 1997*

*AR-010-266*

*June 1997*

**APPROVED FOR PUBLIC RELEASE**

# Resonance Testing of the Gnome Combustor Liner

## Executive Summary

The combustor liner of the Rolls-Royce Gnome engine, which powers the Sea King Helicopter, is known to suffer from cracking of the splitter vane. The effects of this cracking are a reduction in efficiency of the combustor and the possibility of turbine blade damage when pieces of the splitter vane break off entirely and pass through the engine. As part of an investigation into the occurrence and cause of the cracking a series of strain measurements and resonance tests were carried out on an undamaged combustor.

One possible reason for the fatigue of the splitter vane is that a resonant frequency of the vane coincides with a significant mechanical or aerodynamic excitation frequency. The focus of the first part of the experimental work detailed in this report was a modal analysis of the splitter vane including the identification of numerous mode shapes and their associated natural frequencies. The measurement of dynamic strains in the previously observed area of splitter vane cracking enabled these modes to be ranked according to which are most likely to be the cause of cracking assuming a flat excitation frequency spectrum. The results show that the modes at 1432 Hz and 1280 Hz produce the highest and second highest strain levels respectively.

The second part of the experimental work involved quantifying the effects of an interference fit between the splitter vane and another component called the splitter ring. The combustor liner splitter *vane* fits inside the splitter *ring* which is attached to the rear frame of the Gnome engine and an interference fit is allowed according to Rolls Royce specifications. In the experience of a number of operators of the Gnome engine, however, such a configuration results in a shorter time to failure of the combustor liner splitter vane. The modal analysis and recording of dynamic strains was repeated for a simulated interference fit. In this case the two modes generating the highest strains were at 1306 Hz and 1367 Hz. These modes have the same basic mode shape pattern as those identified with the vane in the non-interference condition.

The *static* strains produced by the interference fit were also measured and revealed significant tensile strains on the outer surface of the vane in the relevant areas. Cracking is known to initiate on the outer surface of the splitter vane and it is likely that this mean tensile strain is the cause of accelerated failure of the vane in the case where an interference fit is present.

## Author

### **James Dunlop**

Airframes and Engines Division

*Mr Dunlop is a Professional Officer Grade 1 in the Airframes and Engines Division at AMRL Melbourne. He has worked here since February 1996, after completing a Bachelor of Aeronautical Engineering at the University of Sydney. At DSTO he has been working in the area of vibration analysis of aircraft propulsion systems, with emphasis on modal analyses of engine components. Mr Dunlop has recently taken a position with Hawker De Haviland, Sydney.*

---

# Contents

<b>1. INTRODUCTION .....</b>	<b>1</b>
<b>2. BACKGROUND .....</b>	<b>2</b>
2.1 Gnome Combustor Liner.....	2
2.2 Failure analysis.....	3
2.3 Operator and manufacturer modifications .....	4
<b>3. EXPERIMENTAL METHOD .....</b>	<b>4</b>
3.1 Overview .....	4
3.2 Measurement of natural frequencies and mode shapes .....	6
3.3 Measurement of dynamic strains around combustor liner cut-outs.....	8
3.4 Measurement of static strains around combustor liner cut-outs.....	9
<b>4. DATA PROCESSING AND RESULTS.....</b>	<b>10</b>
4.1 Natural frequencies and mode shapes .....	10
4.1.1 No interference at the splitter vane tangs .....	10
4.1.2 Maximum interference at the splitter vane tangs. ....	11
4.2 Dynamic strain data .....	12
4.3 Static strain data.....	13
<b>5. DISCUSSION.....</b>	<b>14</b>
5.1 Mode shape classification .....	14
5.2 Modes which produce the highest strains near the cut-outs.....	16
5.3 Temperature effects.....	18
5.4 The effect of interference on static strain .....	19
<b>6. CONCLUSIONS .....</b>	<b>20</b>
<b>7. ACKNOWLEDGMENTS .....</b>	<b>21</b>
<b>8. REFERENCES.....</b>	<b>21</b>
<b>APPENDIX A: DIAGRAMS OF MODE SHAPES - NO INTERFERENCE.....</b>	<b>23</b>
<b>APPENDIX B: DIAGRAMS OF MODE SHAPES - INTERFERENCE.....</b>	<b>29</b>

## 1. Introduction

The combustor liner of the Rolls-Royce Gnome engine, which powers the Sea King Helicopter, is known to suffer from fatigue cracking of the splitter vane (see Figure 1). The cracking and subsequent detachment of a piece of splitter vane may affect the operation of the combustor and has been the cause of turbine blade damage. As part of an investigation into the occurrence and cause of the cracking a series of strain measurements and resonance tests were carried out on an undamaged combustor.

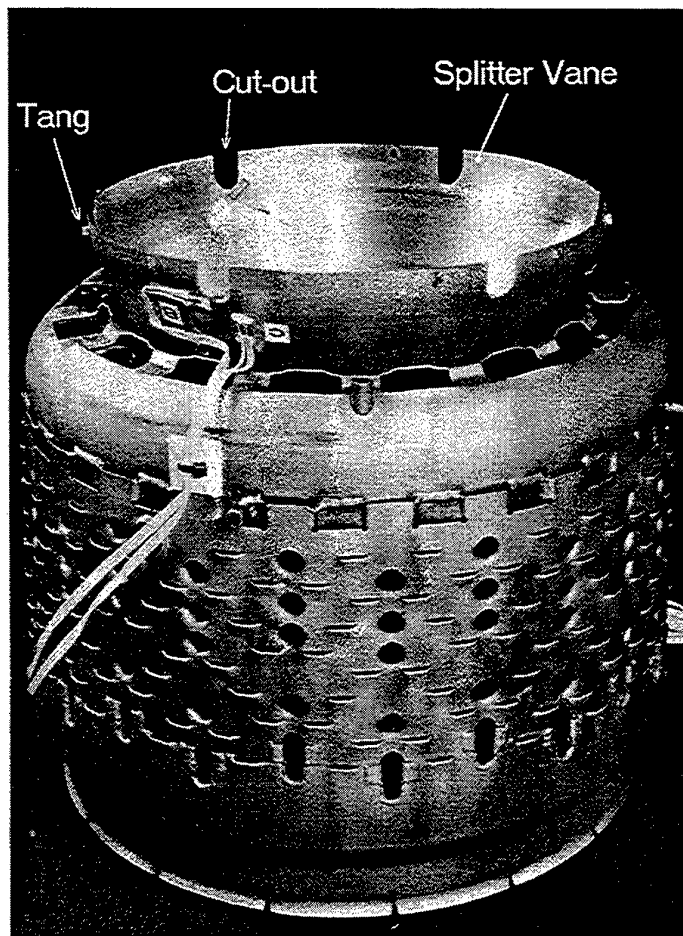


*Figure 1: Gnome combustor liner (showing strain gauge attachment).*

Previous inspections of cracked combustor liner splitter vanes at the Aeronautical and Maritime Research Laboratory (AMRL) have indicated that the failure is due to fatigue of the vane material [1 & 2]. A possible cause of this material fatigue is mechanical or aerodynamic vibratory excitation of the splitter vane at a resonant frequency.

The focus of the experimental work detailed in this report was a modal analysis of the splitter vane and the assessment of which modes of vibration are most likely to cause cracking.

The results were also used to provide some validation of a finite element model analysis [3]. The purpose of this analysis was to investigate the sensitivity of the combustor's structural characteristics to drawing changes and tolerances.

The third phase in the overall assessment of the cracking problem will be the recording of vibration levels from an operational engine.

## 2. Background

### 2.1 Gnome Combustor Liner

The Rolls-Royce Gnome engine is an axial flow turboshaft engine with a gas generator section and a mechanically separate power turbine section. The combustor liner is situated behind the gas generator compressor and is designed to allow efficient burning of the fuel/air mixture while containing the combustion process and preventing overheating of the engine's inner and outer casing. A schematic drawing of a complete Gnome combustor liner is shown below in Figure 2. The splitter vane is located at the forward end of the combustor liner and when the engine is assembled, it projects into the engine rear frame. The splitter vane fits concentrically inside the splitter ring which is welded to the trailing edge of the rear frame radial struts. There are six U-shaped cut-outs on the forward edge of the splitter vane which allow it to clear the radial struts of the rear frame. An annular air gap is maintained between the splitter vane and splitter ring by 12 small tangs welded around the circumference of the splitter vane forward edge. A maximum interference fit of 1mm on the diameter between the tangs and the splitter ring is specified by Rolls Royce drawings.

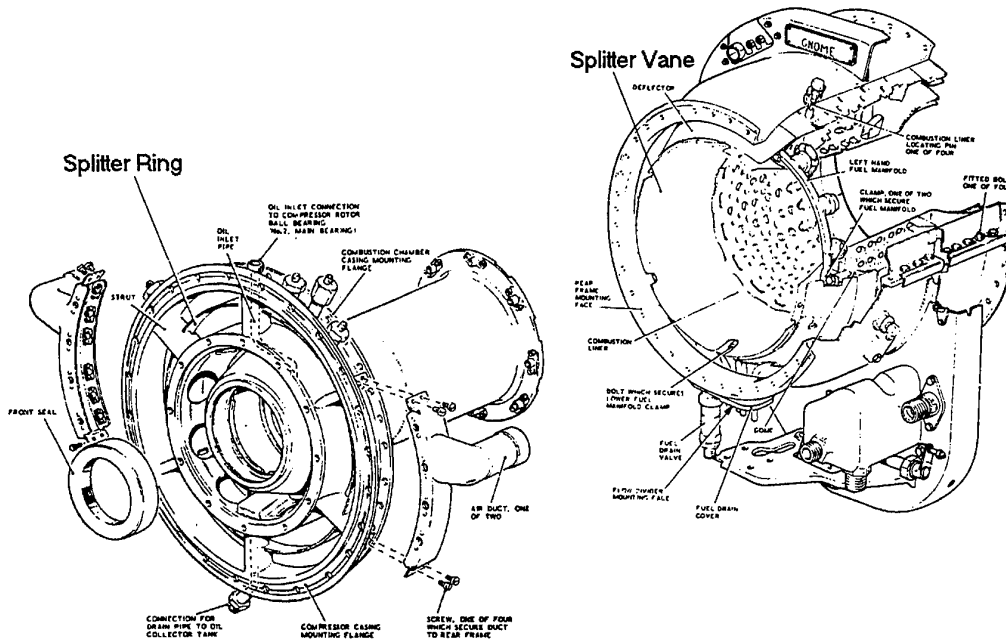


Figure 2: Schematic drawing of the hot section of the Gnome engine.

The purpose of the splitter vane and ring is to divide the air flow from the compressor into three annular regions. Air flow over the outside of the splitter ring goes to the outside of the combustor liner; air flow over the inside of the splitter vane goes to the inside of the combustor liner; and the air gap between the ring and vane meters the air flow to the combustor liner dome, which is the primary combustion zone (see Figure 2).

## 2.2 Failure analysis

Two cracked combustor liners have so far been examined at AMRL and details of these investigations are given in References 1 and 2. Cracking of the splitter vane initiates on its outer surface at the edge of the U-shaped cut-outs, and in a circumferential region around the cut-outs where the surface has been sensitised by excessive electropolishing. The crack propagation is characteristic of vibratory fatigue. In all cases initiation is from the outer surface of the vane indicating the presence of some average tensile stress on the outer surface in addition to any oscillating stress from fatigue loading. This average tensile stress is probably due to an average applied load rather than a manufacturing residual stress, since such residual stresses should have been eliminated by heat treatment processes applied after welding of the vane to the combustor.

## 2.3 Operator and manufacturer modifications

As reported in Reference 4, a number of operators of Gnome and related General Electric (GE) T58 engines around the world have observed cracking of the combustor liner splitter vanes and steps have been taken by both the operators and manufacturers to alleviate the problem. GE added doublers around the cut-outs, to avoid a resonance at flight idle power. Improvements to surface finish around the cut-outs have been tried. The cut-out shape has been changed from a 'U' to 'V' shape. Rolls Royce have recently redesigned the splitter area to eliminate cut-outs and stiffen the conical members.

For the existing design, component manufacturing and build tolerances have been changed to minimise the likelihood of an interference fit between splitter vane (tang) and splitter ring. The presence of an interference fit has been associated with an acceleration of the cracking by some operators of the engines [4].

# 3. Experimental method

## 3.1 Overview

A series of three experimental investigations were undertaken on a complete Gnome combustor liner. The serial number of the combustor liner test article was L2/2997 Q2 and the part number was 573441P01. The average thickness of the vane was measured using a micrometer to be 0.91 mm (0.036"). In all cases the combustor liner was held in a rigid steel assembly (see Figure 3) and support for the combustor liner was provided by four radial pins. In the engine, the support system includes these four radial pins which provide location of the forward end of the combustor in the axial and transverse directions. In addition when assembled in the engine the rearwards facing end of the combustor liner slides over two annular rings and these provide transverse support without imposing an axial restriction which would constrain the thermal expansion of the combustor liner. The experimental rig did not provide any support at the combustor's rearward end.

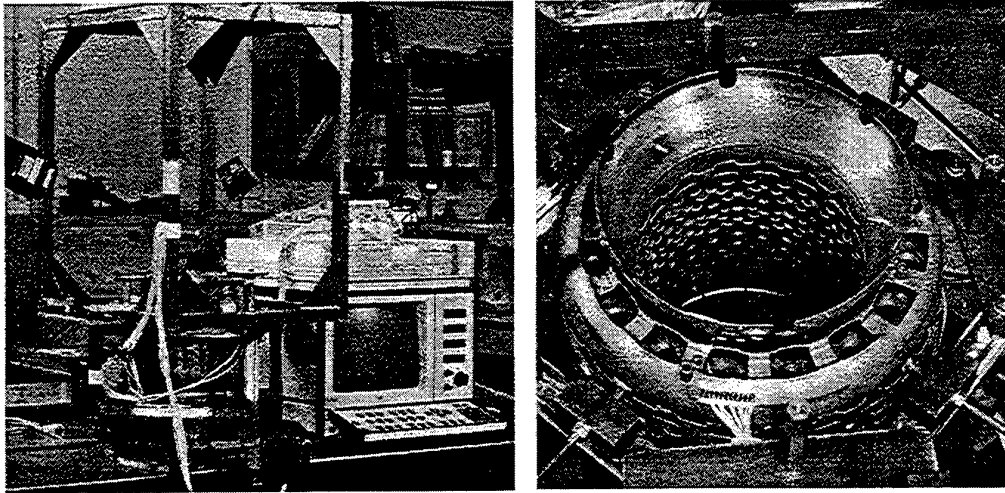


Figure 3: Detail of the combustor liner installed in the support rig.

The first series of tests consisted of a modal analysis of the splitter vane, including the measurement and calculation of natural frequencies and mode shapes. The splitter vane was tested in two configurations simulating either a clearance or interference fit at the 12 tangs around the vane lip. A jig, comprising a steel hoop with 12 radial screws, was used to apply the interference fit to the splitter vane (see Figure 4). Each of the screws contacted one of the tangs and the amount of interference was selected by measuring the gap between the steel hoop and vane outer surface with a pair of vernier callipers. The steel hoop could be considered a fixed reference since it was bolted to the main support rig. It should be noted that using vernier callipers, the best accuracy that could be attained for setting the amount of interference was  $\pm 0.001''$ . The applied interference was  $0.020''$  ( $0.5\text{mm}$ ) at each of the tangs so the relative accuracy was  $\pm 5\%$ .

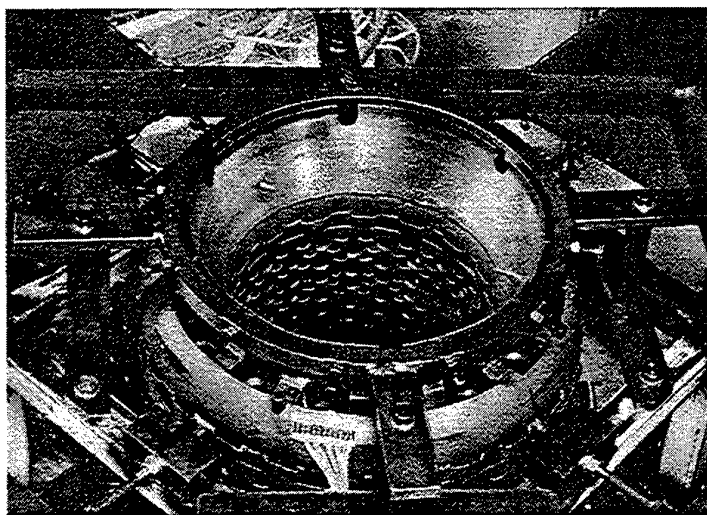


Figure 4: Detail of the steel hoop used to apply an interference fit to the splitter vane.

The second series of tests involved the measurement of dynamic strains in regions close to some of the vane cut-outs. The vane was again tested in the two configurations mentioned above.

The third test concerned the measurement of static strains around the cut-outs with the maximum interference level applied to the splitter vane tangs.

### 3.2 Measurement of natural frequencies and mode shapes

The modal analysis of the splitter vane consisted of measuring its natural frequencies and mode shapes. Mode shapes were defined by measuring the response around the circumference of the forward edge of the splitter vane in the direction perpendicular to the vane surface (see Figure 5). A total of 62 points were surveyed. Response measurements were made using a laser vibrometer which measured the instantaneous velocity of the surface in the direction of the impinging beam. The support rig was mounted on a rotary table and the laser vibrometer mounted on a translating stage. By adjusting the position of the support rig, the central axis of the combustor liner was made to coincide with the axis of rotation of the rotary table. The circumferential position of the laser beam on the circular vane was selected by indexing the rotary table. The two orthogonal linear movements of the translating stage allowed selection of the axial position of the laser beam on the vane and also enabled focusing of the laser beam to produce the strongest possible signal. All the hardware was bolted to the surface of a large vibration-isolated table which had pneumatic supports.

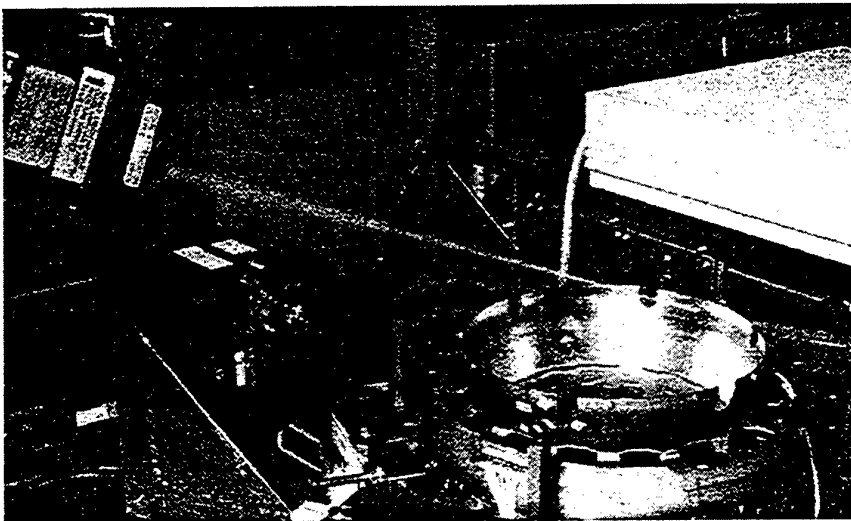


Figure 5: Measurement of vane response using the laser.

A number of excitation methods were tried including the use of an electromagnetic shaker, an acoustic speaker and an instrumented hammer. The method which

produced the best quality data was impact excitation with an instrumented hammer and the results given in this report were obtained using this method.

To conduct a modal analysis of a structure with numerous degrees of freedom, in most cases, it is sufficient to keep the excited degree of freedom constant and measure the response at all degrees of freedom. Alternatively the degree of freedom at which the response is measured can be kept the same and the excitation source moved to all degrees of freedom. For these first experiments the point of impact excitation was kept the same and the response of the vane in all the desired degrees of freedom was measured using the laser by indexing the rotary table. A total of 62 points were used corresponding to 5 degree increments around the vane circumference, with the exception of those positions where vane cut-outs or the obstruction of the laser by the support rig required a 10 or 15 degree increment.

It is usual for the excited degree of freedom to also be a degree of freedom for which the response is measured - giving a so-called driving point measurement - but this was not possible for reasons which are explained here. One requirement of impact excitation is that the force pulse produced on impact should be of sufficiently short duration that the level of excitation provided at the highest frequency of interest is no less than 20dB below the DC excitation level [5]. It was found that, even using the lightest possible hammer with the hardest tip, the compliance of the splitter vane was such that impacting at the desired point of the response measurement (i.e. at the vane's forward edge) produced an impact pulse of relatively long duration and excitation was limited to a maximum frequency of approximately 500 Hz. Initial experimentation revealed a requirement for a frequency range of 2 kHz to cover all the modes of interest. Consequently a point on the vane surface was chosen which was nearer to the supporting structure of the rest of the combustor liner and therefore less compliant, resulting in a shorter pulse with the necessary frequency content.

The response and excitation signals were fed into a frequency analyser and frequency response spectra calculated before being down-loaded to a computer data acquisition system. Response spectra for all 62 positions around the circumference of the vane forward edge were collected and the natural frequencies identified from peaks in the  $H_2$  frequency response function [6].

The mode shapes were determined using the method of quadrature picking [7]. It should be noted that this method assumes implicitly that the value of the response function at the resonant frequency of a particular mode is determined purely by that mode and not influenced by other nearby modes. This assumption is valid provided the modal peaks are well separated in terms of frequency. Although the response spectra for the splitter vane exhibited some closely spaced modes the experimental data was intended to be used for a mainly qualitative analysis and it was decided that this use did not warrant the implementation of a more accurate but also more complex multi-degree of freedom curve fitting procedure for the identification of modal parameters.

### 3.3 Measurement of dynamic strains around combustor liner cut-outs

Cracking of the splitter vane is known to initiate at the edge of the U-shaped cut-outs or in a region close to these cut-outs. For this reason the next step in the experimental testing was to strain gauge the splitter vane at the cut-outs and measure the dynamic strain response to a broad-band excitation. From these measurements, it was possible to determine which of the previously identified modes of vibration generate the largest strain amplitudes and are therefore most likely to be the cause of cracking.

A total of 12 strain gauges were attached to the splitter vane. The gauges were distributed at two cut-outs as shown in Figure 6. Strain gauging of all the cut-outs would have been ideal but the added complexity of attaching more gauges and collecting the data from all of them was not warranted. The choice of which cut-outs to strain gauge and of the appropriate position and orientation of the gauges at the chosen cut-outs was based on the observed location and orientation of cracks on one of the failed splitter vanes examined at AMRL.

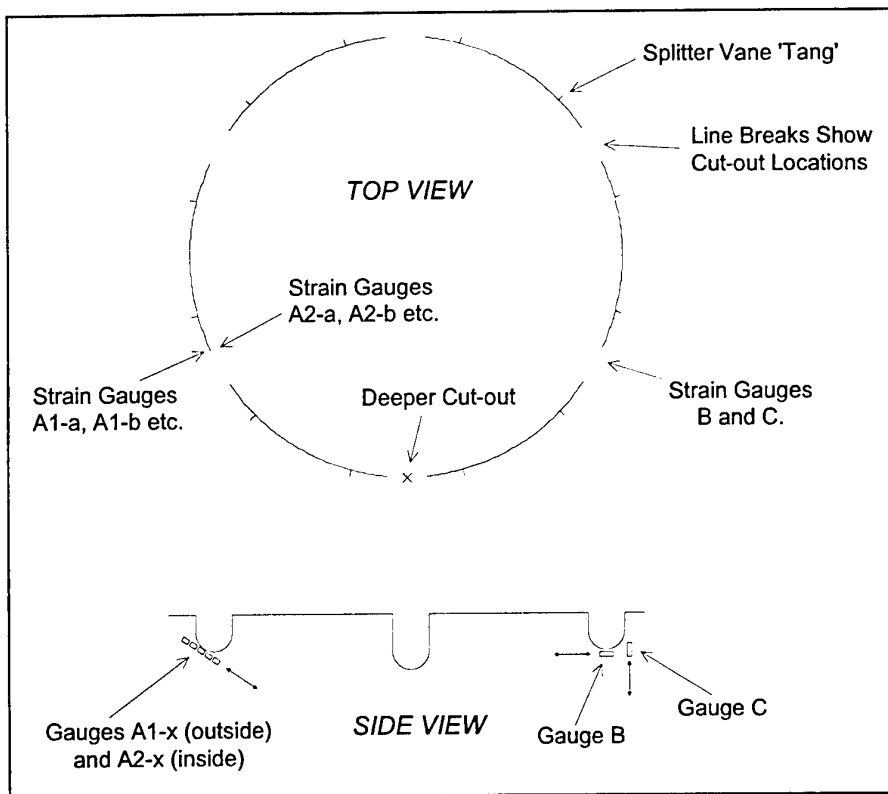


Figure 6: Schematic drawing of the strain gauge locations on the splitter vane.

Broad-band excitation was again provided by an instrumented hammer, but for these experiments the point of response measurement was fixed (i.e. one of the strain gauges was the response transducer) and a complete survey of the splitter vane's dynamic

response required the movement of the point of impact excitation. The purpose of taking measurements from the splitter vane with numerous points of excitation was not, in this case, to obtain a description of the mode shapes (although this was achieved by default). Rather, it was necessary to provide equal excitation for all modes and this could only be achieved by having a 'roving' point of excitation. If only one point of excitation was used then those modes which happened to have a nodal line close to or coinciding with the point of impact would not have been excited.

The aim of exciting all modes equally was to determine which of them caused large strain at the cut-outs because of their deformation shape and not as a result of which mode was most readily excited for a particular point of impact. To achieve this, numerous excitation points were used and *for a certain mode* the values of the frequency response function *at that modal frequency* were tabulated. The maximum value would correspond to the response measured when the vane was impacted at an anti-nodal line *of that mode* and this value was used for comparison with the strains produced by other modes. To ensure that excitation was provided close to the anti-nodal lines of all possible modes, a total of 72 response measurements were made corresponding to impacting the vane at 5 degree increments around its circumference.

The complete set of 72 measurements were made for only two of the 12 possible strain gauges; namely gauges A1-b and B (see Figure 6). The other gauges were used only for static measurements (see Section 3.4). Gauges A1-b and B were chosen for the dynamic measurements because they were on the outer surface of the splitter vane (where cracks are known to initiate) and were close to the edge of the cut-outs. The strain gauge signals were fed into a strain gauge conditioner and amplifier system and then into a frequency analyser. Quarter bridge circuits were used because temperature effects were not of concern for the collection of high frequency dynamic data.

### **3.4 Measurement of static strains around combustor liner cut-outs.**

The last of the experimental tests to be performed on the splitter vane was a measurement of the static strains generated in the regions around the cut-outs with application of the maximum drawing interference. As previously mentioned, the experience of operators of the Gnome engine indicates an acceleration of the cracking problem with an interference rather than clearance fit and it was of interest to quantify the effects of this change on the strain levels.

Data from the complete set of 12 gauges, at the 2 cut-outs, were collected. As with the dynamic testing, quarter bridge circuits were utilised. No allowance was made for temperature changes, but the test was of short duration and any errors were not expected to be significant.

## 4. Data processing and results

### 4.1 Natural frequencies and mode shapes

The process of determining natural frequencies and mode shapes required the identification of peaks in the frequency response spectra ( $H_2$ ) and tabulation of the values of all peaks at all measurement points. As a consequence of the large amount of data collected, this task was performed on a computer using the MATLAB software package. A peak-finding algorithm was employed which only registered peaks as being valid if they were present for more than 40% of the total number of spectra (which were recorded at the different measurement points). The purpose of this procedure was to avoid the tabulation of large numbers of peaks, which rather than being a representation of a mode, were in reality noise spikes. A side effect was that modes which were 'weak' were also rejected, but it is to be expected that modes which are not readily excited do not generate significant strains.

#### 4.1.1 No interference at the splitter vane tangs

A total of 23 modes were identified when there was no interference applied to the vane tangs. The lowest frequency mode is at 456 Hz and the highest at 2040 Hz. The limit on the highest frequency mode that could be identified was determined by the drop off in excitation levels above 2 kHz.

Figure 7 shows an example of two of the modes including the natural frequency values and accompanying graphical representations of the mode shapes. The six cut-outs of the splitter vane are shown on the diagrams by breaks in the lines representing the vane lip. The deeper cut-out is marked with a cross and the tangs are shown by small radial line segments. Note that the mode shapes are scaled arbitrarily and the absolute amount of deformation on the figures has no physical significance. Figures showing the complete set of modes are given in Appendix 1.

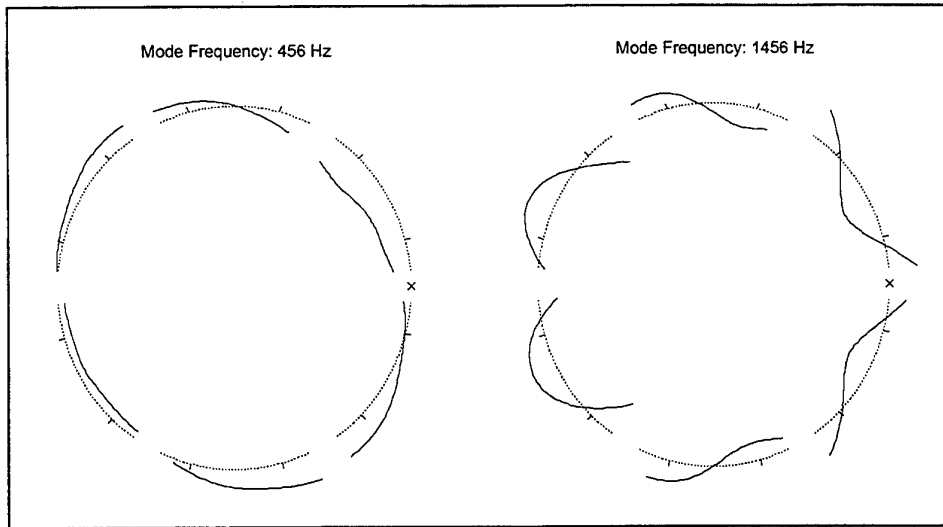


Figure 7: Two of the splitter vane modes - no interference applied.

#### 4.1.2 Maximum interference at the splitter vane tangs.

With the maximum interference of 0.5mm (0.020") applied at each of the vane tangs, 14 modes were identified ranging in frequency from 1153 Hz to 1775 Hz. Figure 8 shows two of these modes and the complete set are included in Appendix 2.

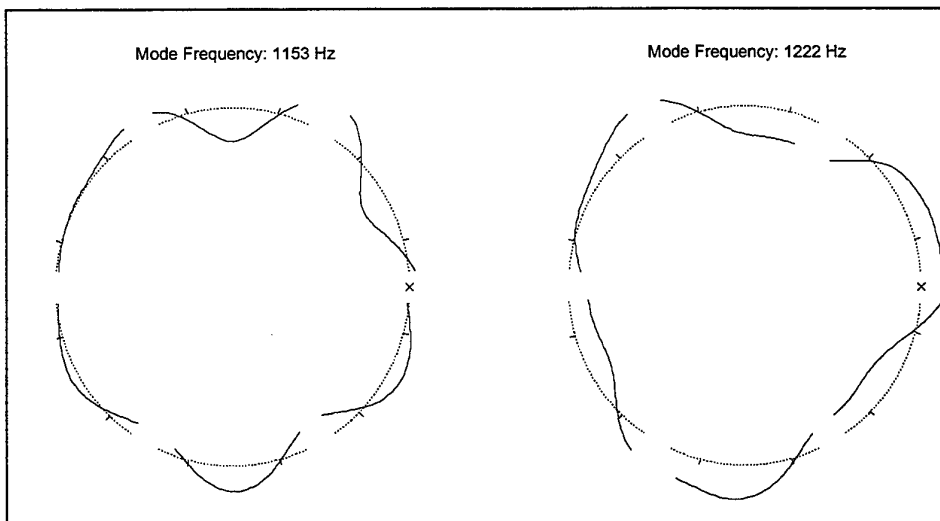


Figure 8: Two of the splitter vane modes - interference applied.

The interference fit between the screws attached to the steel hoop and the tangs ensured positive contact and when excited the amplitude of displacement caused by the vibrations was not sufficient to allow loss of contact at the tangs. It would therefore be expected that the mode shapes all show zero displacement at the tangs. This is not

the case because the response was not measured precisely at the same axial level as the tangs but slightly below, and mode shapes such as the one at 1222 Hz exhibit displacement at some of the tang locations (see Figure 8).

### 4.2 Dynamic strain data

Figures 9 and 10 show a comparison of the strains at the splitter vane cut-outs for most of the modes illustrated in Appendices 1 and 2. The horizontal axes on the graphs give the modal frequencies and the heights of the bars represent the normalised strain measured at the corresponding modal frequency. Not all the modes are shown on these graphs because for some of them the strains recorded at the cut-outs were relatively small and therefore not of interest. The vertical axis is labelled as normalised strain since for each mode there were 72 spectra to choose from corresponding to 72 points of excitation and the value shown on the graph was the maximum for that mode from the 72 spectra.

Units for the normalised strain are not given since the mode shapes were not scaled and the dynamic strain readings were not calibrated. The operational excitation forces are not able to be determined in absolute terms and so there is no reason to calculate the strain per unit force in engineering units. It is only useful to have a relative measure of strains produced by each of the modes given an equivalent application of excitation force at each of the modal frequencies. Note that this equivalence assumes not only an equal magnitude of force excitation but that each mode was excited at a point where its movement is greatest (i.e. at an anti-node).

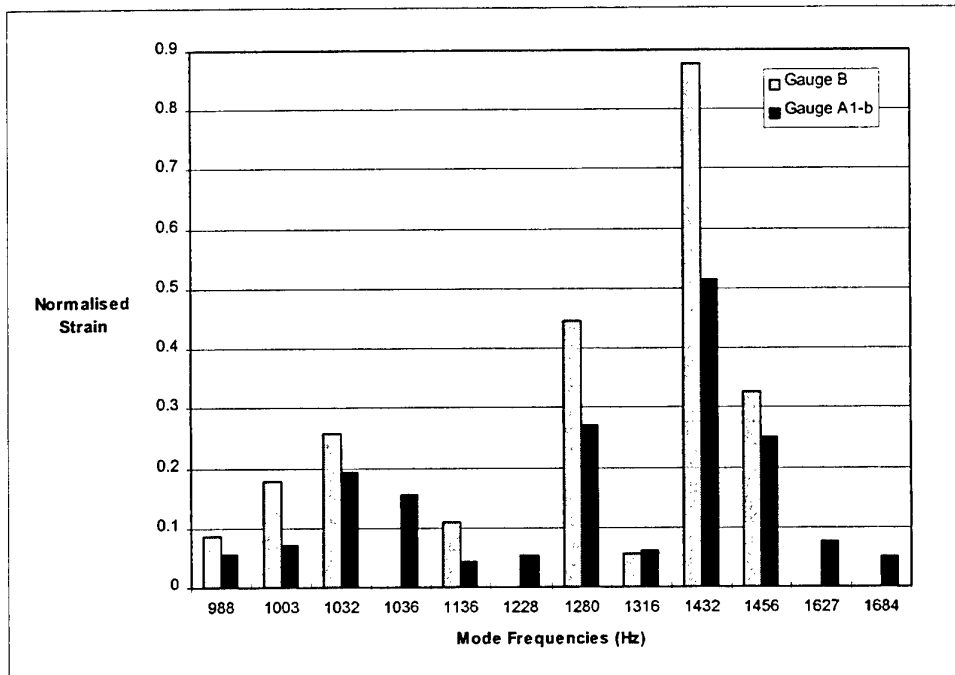


Figure 9: Cut-out strain comparison for non-interference modes.

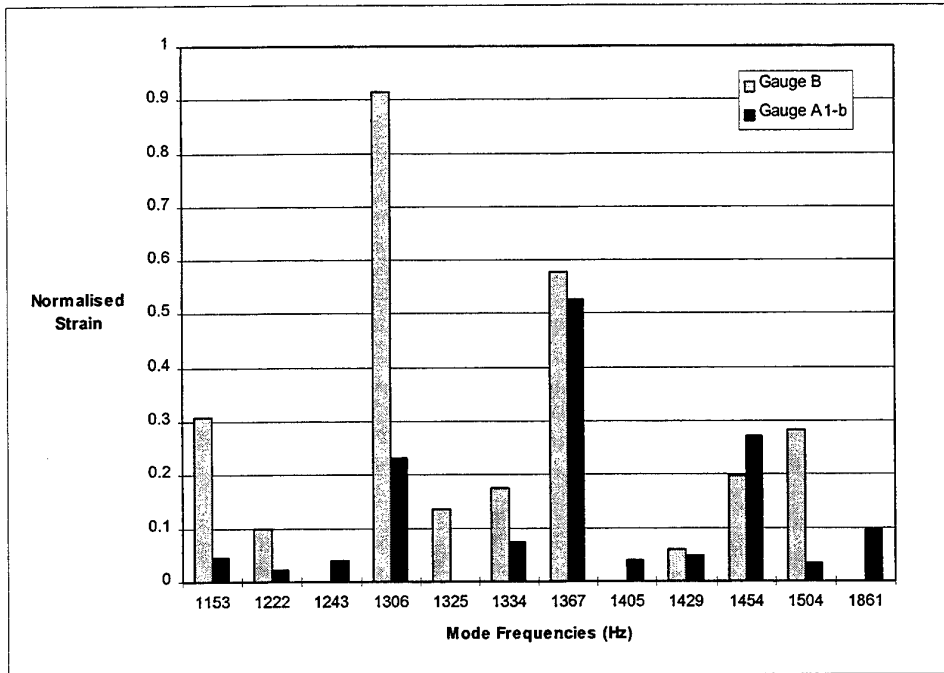


Figure 10: Cut-out strain comparison for interference modes.

### 4.3 Static strain data

Table 1 shows the static strains measured when the splitter vane was subjected to the maximum allowable interference of 0.5 mm (0.020") at each tang.

Table 1: Static strain readings with maximum interference at the vane tangs.

Gauge Number	Microstrain ( $\mu\epsilon$ )	Gauge Number	Microstrain ( $\mu\epsilon$ )	Gauge Number	Microstrain ( $\mu\epsilon$ )
A1-a	1180	A2-a	-1540	B	1390
A1-b	1460	A2-b	-2160	C	1070
A1-c	1250	A2-c	-2540		
A1-d	840	A2-d	-2200		
A1-e	400	A2-e	-1570		

Figures 11 and 12 show graphs of the trend in strain data along gauge rows A1 and A2. These graphs indicate that along the line of measurement of the gauges, the local strain maximum was captured. Clearly, however, no conclusions can be drawn about the actual local maximum of principal strain.

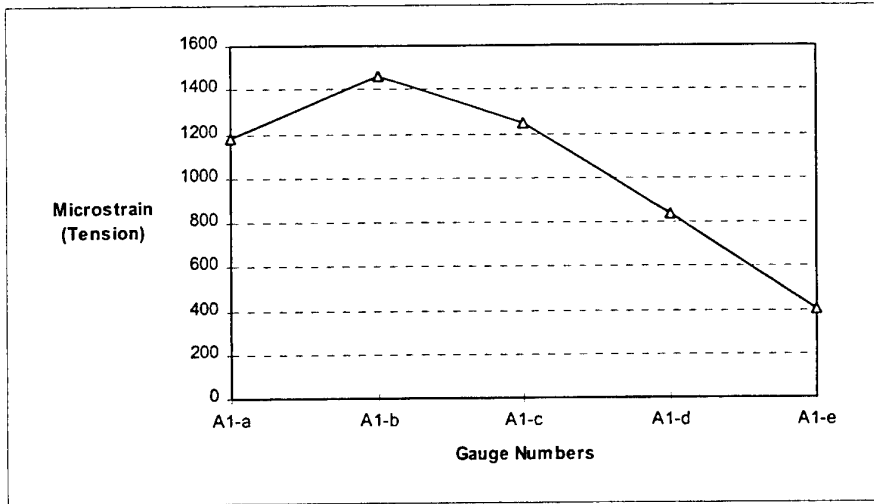


Figure 11: Strain variation along the A1 row of gauges.

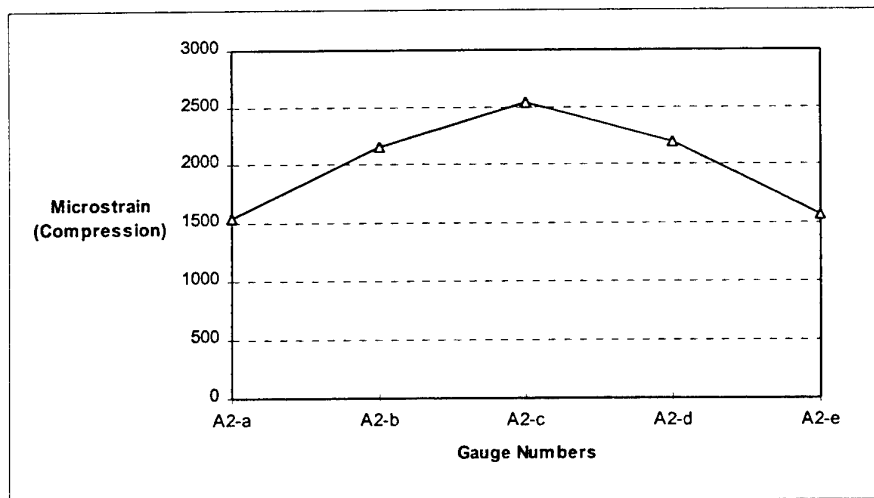


Figure 12: Strain variation along the A2 row of gauges.

## 5. Discussion

### 5.1 Mode shape classification

It is useful to apply some method for classifying the mode shape results, particularly for the purpose of comparing the experimental mode shapes and natural frequencies in this report with the finite element model results given in Reference 3. The splitter vane is an annulus which is close to being axi-symmetric and as a consequence the most simple means of classifying a mode is to count the number of lobes of the deformed shape which extend outside the undeflected profile of the splitter vane. For example,

Figure 13 shows a 2 lobe and a 3 lobe mode, designated as modes  $n=2$  and  $n=3$  respectively (where  $n$  is equal to the number of lobes).

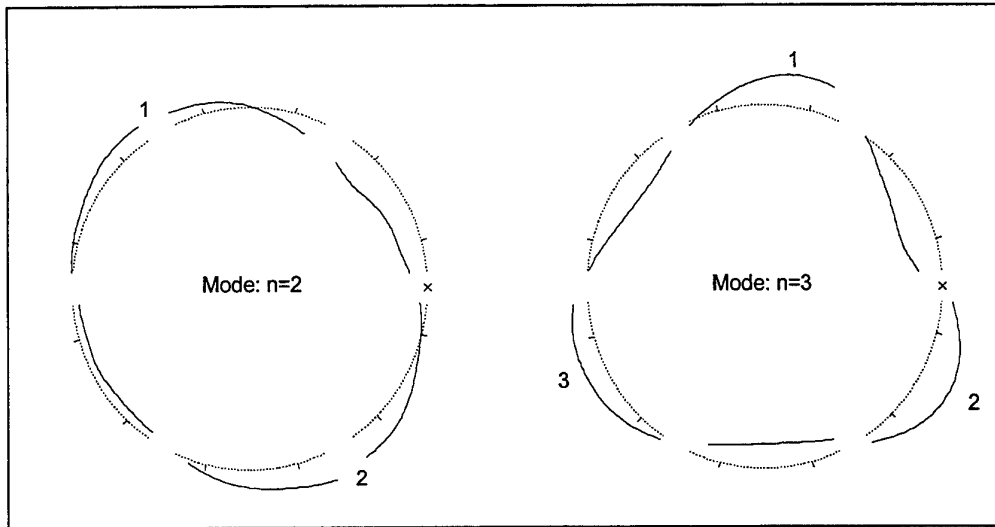


Figure 13: Classification of modes according to lobe number.

Listed in Tables 2 are the modal frequencies and the corresponding classifications according to this scheme. For a given number of lobes there are, in most cases, several modes.

Table 2: Mode classification according to the number of lobes.

Number of Lobes $n$	Mode Frequencies (Hz) - No Interference				
	(a)	(b)	(c)	(d)	(e)
2	456	488			
3	988	1524			
4	876	880	920		
5	1032	1036	1184		
6	1136	1280	1316		
7	1432	1456			
8	1592	1648	1684	1748	1772
9	2040				
	Mode Frequencies (Hz) - Interference				
	(a)	(b)			
6	-	1306			
7	1367				

Although 14 modes were identified from the experimental data for the splitter vane in the interference fit condition, only 2 of these are listed in Table 2. Unlike the results without interference, most of these 14 modes did not exhibit deformation shapes with similar amplitudes of deflection at each of the lobes around the circumference. For example, Figure 14 shows a comparison of a typical mode shape without interference and another with interference.

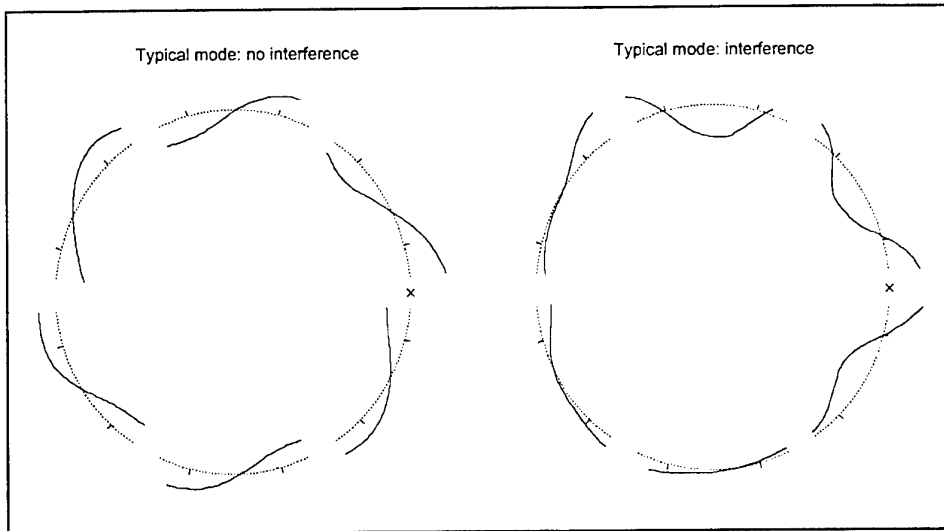


Figure 14: Comparison of interference and non-interference mode shapes.

The circumferential asymmetry of many of the mode shapes for the interference case renders the classification by lobe number rather meaningless. Furthermore the purpose of classification is mainly to allow validation of the *non-interference* results from the finite element model [3]. The reason for the asymmetry of many of the interference case modes is not well understood but may be a result of variation in the damping provided by the screws which contact the tangs.

## 5.2 Modes which produce the highest strains near the cut-outs

The two modes which *are* listed in Table 2, for the case of an applied interference, are those which generate the two highest strains at the cut-outs as shown in the bar graphs of Figures 9 and 10. The *a* and *b* classifications of these modes as  $n=6b$  and  $n=7a$  were given by matching the mode shapes with their counter parts for the non-interference case (see Figures 15 and 16). If the marked asymmetry of the interference case modes is ignored then the basic patterns of the mode shapes can be seen to be the same. It is interesting but not very surprising that the modes which generate the two highest strains in the non-interference case also generate the two highest strains in the interference case. These two modes, in the non-interference case, have nodes at, or close to, each of tangs and therefore by applying a rigid constraint at the tangs with the simulation of an interference fit it is to be expected that the modes would still be

present albeit at slightly different frequencies. Furthermore if they generate the two highest strains without interference and can persist with interference, which effectively stiffens the splitter vane, it is logical that they should generate the highest strains in this case also.

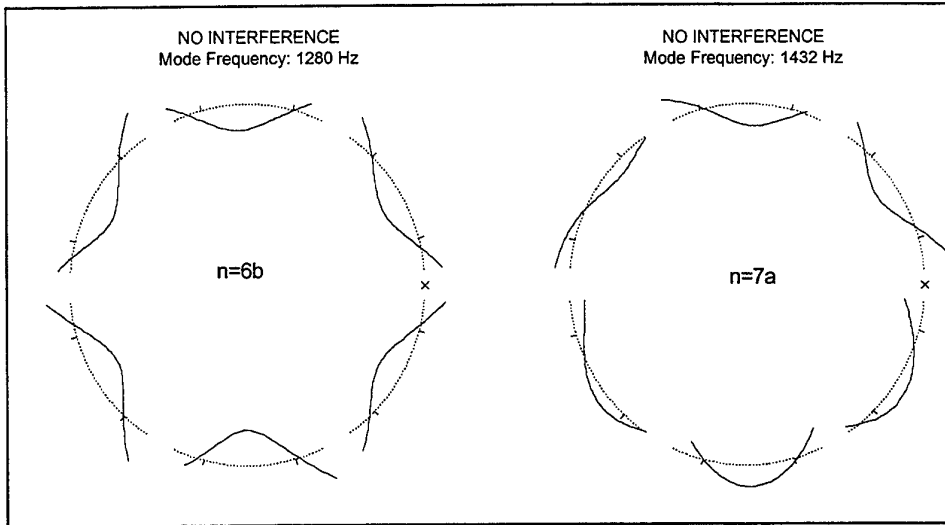


Figure 15: Non-interference modes which generate the two highest cut-out strains.

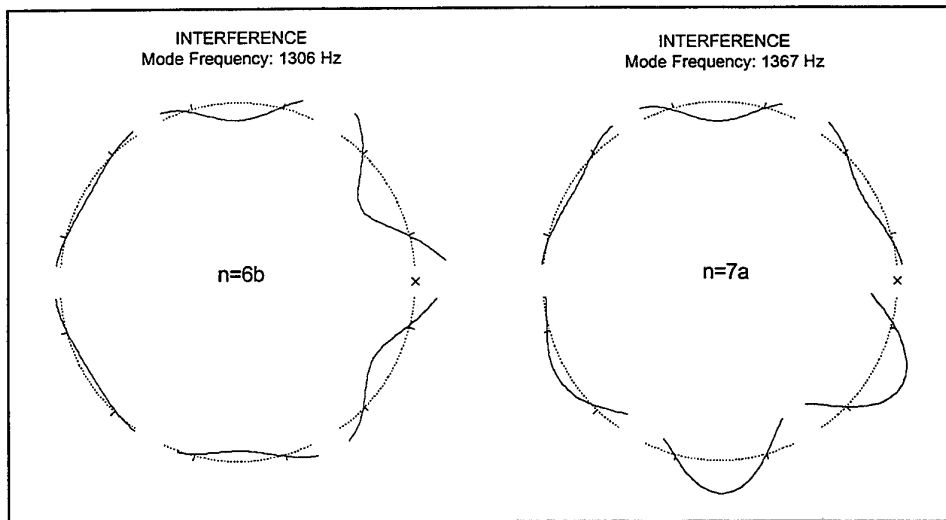


Figure 16: Interference modes which generate the two highest cut-out strains.

The modes  $n=6b$  and  $n=7a$  therefore, in both the interference and non-interference cases, are a focus for attention. Although other modes exist which cause significant strains, the maximum strain produced by one or the other of these two modes is approximately twice the level produced by any other mode, and for this reason, they are the most likely cause of a resonance problem, if one exists.

It is interesting to note that the natural frequencies of these modes are relatively close to each other, and are contained in a band from 1280 Hz to 1432 Hz for both the interference and non-interference cases. This band defines a narrow range of frequencies for which a vibratory excitation could cause a damaging resonant response. These values should only be taken as an approximate guide since manufacturing variations between splitter vanes will inevitably lead to variations in natural frequencies.

It is also interesting that the maximum strain level produced at the cut-outs is very similar regardless of whether an interference fit is imposed on the splitter vane or not. With interference and without interference the maximum strain values are 0.88 and 0.91 respectively (for the modes with natural frequencies of 1432 Hz and 1306 Hz).

### 5.3 Temperature effects

The modal testing detailed in this report was carried out at room temperature, whereas in operation, the splitter vane of the combustor will be subject to a temperature of about 300°C - 350°C. At higher temperatures the Modulus of Elasticity of Hastelloy X decreases and its Poisson's ratio increases (slightly), as shown in Table 3.

Table 3: Variation in Hastelloy X material properties with temperature.

Temperature (°C)	Modulus of Elasticity, E (GPa)	Poisson's Ratio, $\mu$
21	205.0	0.3200
300	184.8	0.3235

The mode frequencies can be adjusted to account for these changes in material properties based on the assumption that the splitter vane vibrates in a manner similar to a simple plate. For plate vibration the dependency of natural frequency on  $E$  and  $\mu$  is given by,

$$\omega \propto \sqrt{\frac{E}{1 - \mu^2}}$$

(see Reference 8). Substituting the values given in Table 3 into the above proportionality - for a change in temperature from 21°C to 300°C the natural frequencies ( $\omega_n$ ) are reduced by 4.9%.

Reference 3, which reports the results of finite element modelling of the Gnome combustor, also quantifies the effects of temperature change on the (computed) natural frequencies of the vane. For the same temperature change, the reduction in frequency values is on average 4.2% which is in reasonable agreement with the analytical prediction given above.

Using a reduction of 4.9% a summary of the adjusted natural frequency values is given in Table 4.

Table 4: Mode frequencies adjusted to account for 300 °C operating temperature.

Number of Lobes n	Mode Frequencies (Hz) - No Interference				
	(a)	(b)	(c)	(d)	(e)
2	434	464			
3	940	1449			
4	833	837	875		
5	981	985	1126		
6	1080	1217	1252		
7	1362	1385			
8	1514	1567	1601	1662	1685
9	1940				
	Mode Frequencies (Hz) - Interference				
	(a)	(b)			
6	-	1242			
7	1300				

#### 5.4 The effect of interference on static strain

It was mentioned previously that the crack initiation on the two splitter vanes examined at AMRL occurred on the outer surface of the vane. This indicates that the oscillating load which causes the cracking produces stresses which are superimposed on an existing tensile stress on the vane outer surface. This may be a residual tensile stress which results from the manufacturing process but it is more likely to be an applied tensile stress caused by the interference fit between the splitter vane and ring.

The static strain measurement results show that high strain levels exist around the splitter vane cut-outs when the maximum drawing interference is simulated. The maximum tensile strain recorded was 1460 microstrain at gauge A1-b (see Table 1). The yield strain of Hastelloy X is 1500 microstrain at the vane operating temperature of approximately 350°C [9].

For a number of reasons, however, the strain values recorded from these tests set the upper limit of the levels that might be produced in practice. Firstly the splitter ring, which contacts the vane to produce an interference fit, is more compliant than the rigid jig used in this experiment and the deformation caused by the interference would be shared between the two components. Secondly the splitter vane used for these tests is

close to the upper bound of the thickness tolerance (0.91mm) and greater thickness implies higher strains for a specified displacement due to interference. The third and most obvious reason is that current practice in the Royal Australian Navy (RAN) is to ensure that the maximum interference level does not occur, by machining the tangs on the splitter vane down to their lower tolerance.

In spite of these comments, it is significant that even the upper limit of the strain values should be so high relative to the material yield point. Any increase in mean tensile stress on a component subject to cyclic loading will reduce its fatigue life and these results suggest a causal link between increase in interference fit and a reduction in splitter vane operating hours before cracking occurs.

## 6. Conclusions

The central purpose of the experiments detailed in this report was to find the modes of vibration of the combustor liner which might be the cause of cracking around the splitter vane cut-outs.

Numerous modes of vibration of the Gnome combustor liner splitter vane were identified. These modes were compared according to the tensile strain they generate around the cut-outs of the splitter vane when all modes are excited equally. The splitter vane was tested in two configurations simulating a clearance and an interference fit of the splitter vane to the splitter ring.

The mode classified as  $n=6b$  at 1306 Hz produces the highest strain in the case where an interference fit is simulated. Without interference, the mode  $n=7a$  at 1432 Hz produces the highest strain. These two modes,  $n=6b$  and  $n=7a$ , generate the highest and second highest strains in both test configurations of the splitter vane.

The range of frequencies for which there is the greatest probability of a damaging resonant response is from 1280 Hz to 1432 Hz. Although exact mode frequencies have been given in this report, these frequencies should only be considered as approximate when matching these with potential excitation frequencies. Considerable variation in the splitter vane thickness is known to occur for different combustor liners (the manufacturer's tolerance allows for a range of thicknesses from 0.635 mm to 0.91 mm).

The difference between the temperature which a combustor liner experiences when it is installed in an operating engine (300 - 350°C) and the temperature at which the modal testing was conducted can be approximately accounted for by reducing the test frequencies by a fixed percentage of 4.9%.

Static strain measurements taken around the splitter vane cut-outs revealed the existence of very high tensile strains on the outer surface of the vane when the maximum allowable interference fit of the splitter ring was simulated. Some of the

measured tensile strains were close to the yield strain of Hastelloy X. The test article strain levels are certainly higher than those generated in practice but the results give a strong indication of why an interference fit could cause accelerated failure of the splitter vane.

It should be emphasised that if resonant vibration is the cause of the fatigue of the Gnome combustor, modes other than those given prominence above may be responsible. The response of the splitter vane to an applied vibration is a function not only of the dynamic characteristics of the vane but also the relative levels of excitation, at different frequencies, which are present in the applied vibration itself. The identification of the problem modes which has been made here assumes that the excitation spectrum is flat, which is unlikely to be the case. A more thorough comparison of the modes would require, in addition, a survey of the operational vibration environment of the combustor.

## 7. Acknowledgments

The author would like to thank Gordon Stocks for his helpful discussions and assistance in preparing this report.

Thanks also go to:

David Dyett for manufacturing the support rig and a number of other components required for the experimental work; Jim Gordon and David Rowlands for their help with issues concerning the laser measurement system; Phil Ferrarotto and Barry Ashcroft for implementing the strain gauging of the combustor liner; and Albert Wong for his advice in many areas and assistance with the preparation of this report.

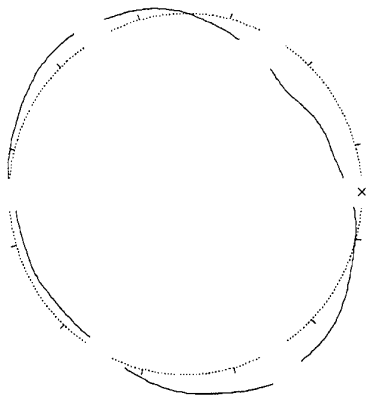
## 8. References

- [1] Athinotis, N. (1996)  
*Sea King Gnome Combustor Liner Splitter Vane Cracking* (DSTO Divisional Discussion Paper 0162).
- [2] Athinotis, N. (1996)  
*Gnome Vane (spin formed SN: 564115)* (AMRL Minute).
- [3] Zhuang, W.Z., Stocks, G.J., and Swansson, N.S. (1997)  
*Stress and Vibration Analysis of the Gnome Combustor Splitter Vane* (AMRL Report in course of publication).

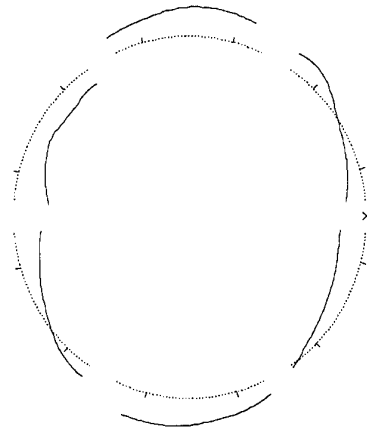
- [4] Bennett, J. (1995)  
*Report on a Visit to the USA, Canada and the UK, October 1995 - Appendix C*  
(AMRL Report Number DST-OSR-0072).
- [5] Døssing, O. (1988)  
*Structural Testing Part I: Mechanical Mobility Measurements*. Brüel & Kjær.
- [6] Ewins, D.J. (1984)  
*Modal Testing: Theory and Practice*. John Wiley & Sons Inc.
- [7] Døssing, O. (1988)  
*Structural Testing Part II: Modal Analysis and Simulation*. Brüel & Kjær.
- [8] Crede, C.E. & Harris, C.M. (1976)  
*Shock and Vibration Handbook (Second Edition)*. McGraw-Hill, Inc.
- [9] *Materials Handbook MIL-HDBK-5E*, 1987.

## Appendix A: Diagrams of mode shapes - no interference

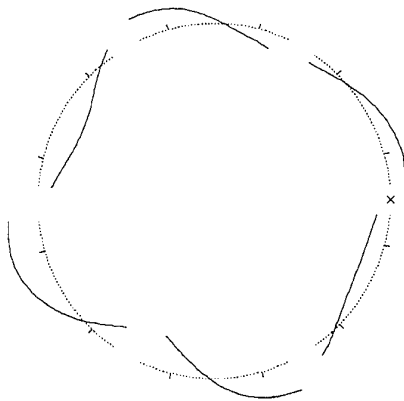
Mode Frequency: 456 Hz



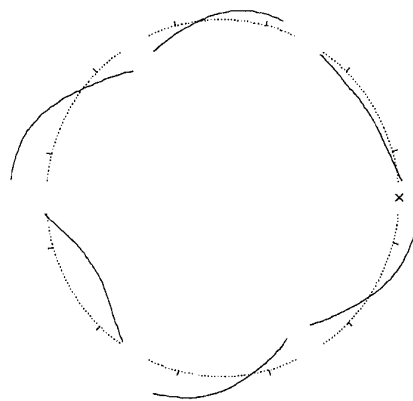
Mode Frequency: 488 Hz



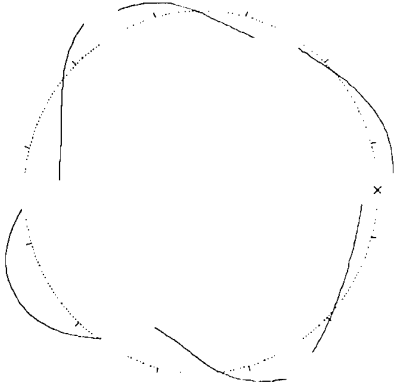
Mode Frequency: 876 Hz



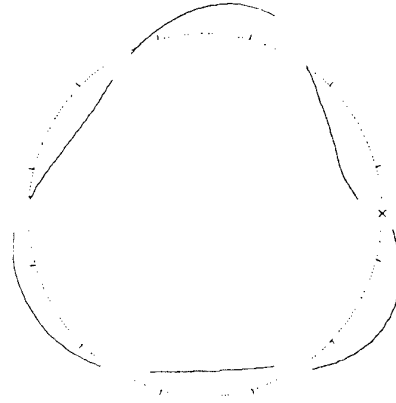
Mode Frequency: 880 Hz



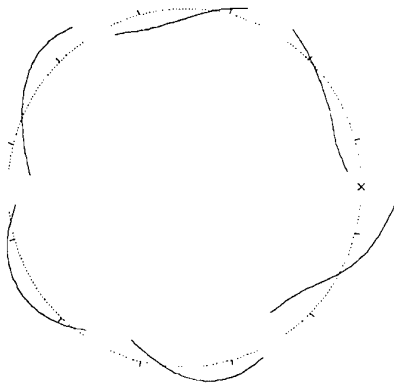
Mode Frequency: 920 Hz



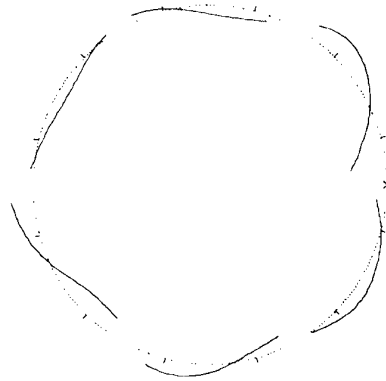
Mode Frequency: 988 Hz



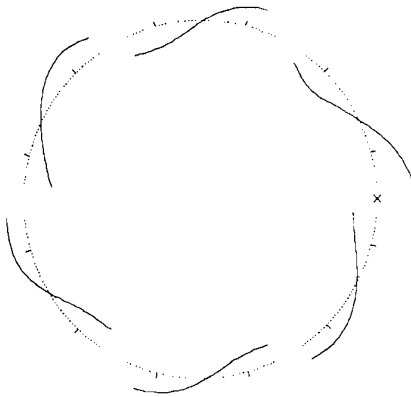
Mode Frequency: 1032 Hz



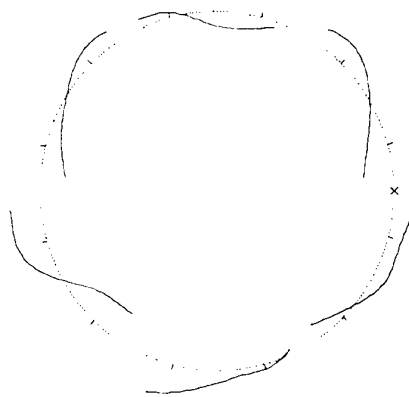
Mode Frequency: 1036 Hz



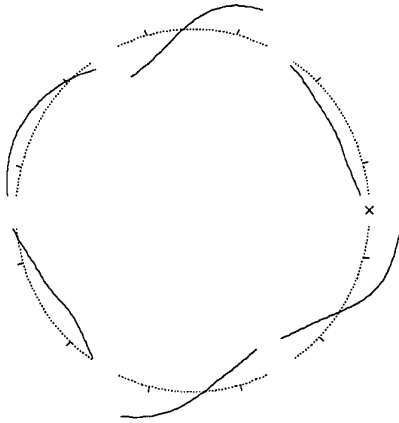
Mode Frequency: 1136 Hz



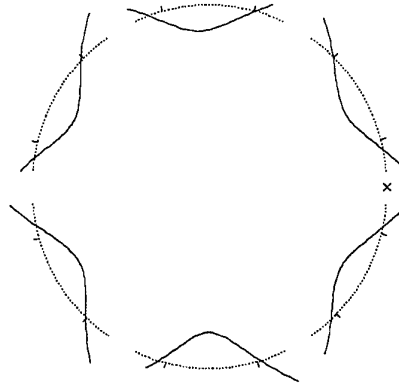
Mode Frequency: 1184 Hz



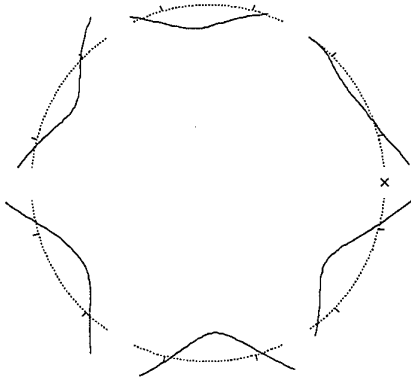
Mode Frequency: 1228 Hz



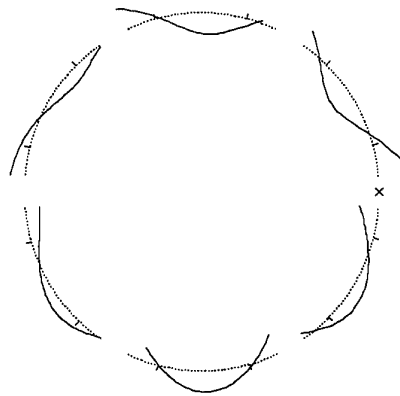
Mode Frequency: 1280 Hz



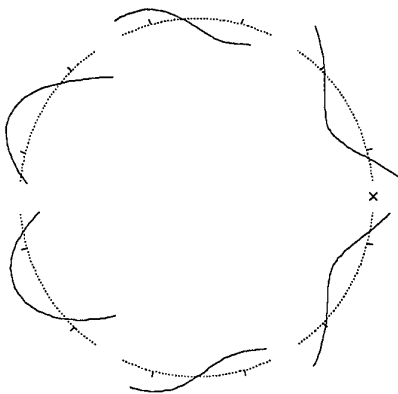
Mode Frequency: 1316 Hz



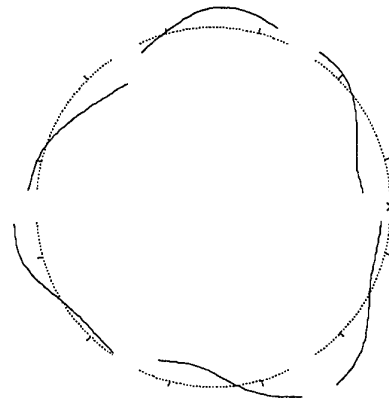
Mode Frequency: 1432 Hz



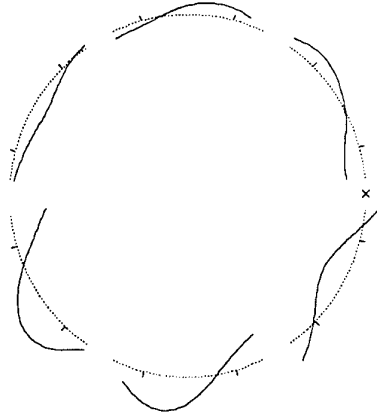
Mode Frequency: 1456 Hz



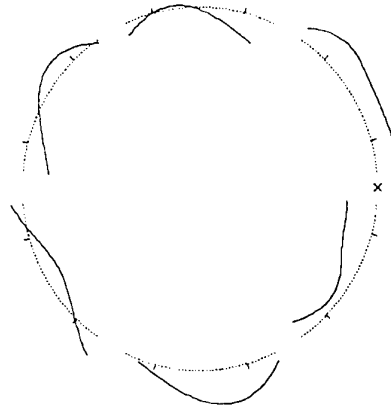
Mode Frequency: 1524 Hz



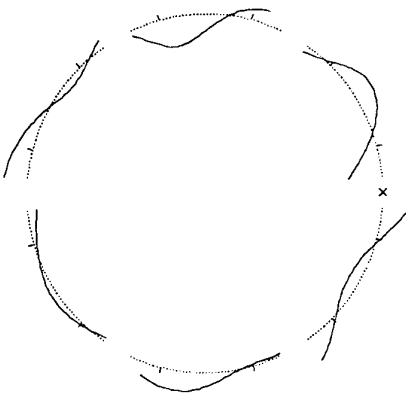
Mode Frequency: 1592 Hz



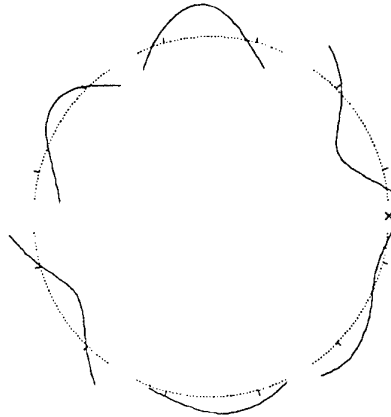
Mode Frequency: 1648 Hz



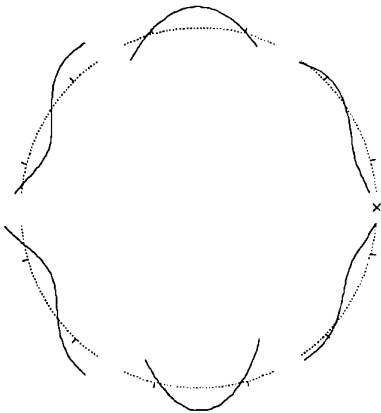
Mode Frequency: 1684 Hz



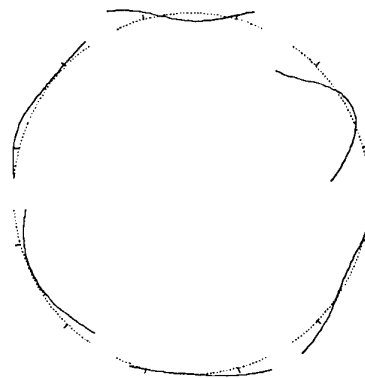
Mode Frequency: 1748 Hz



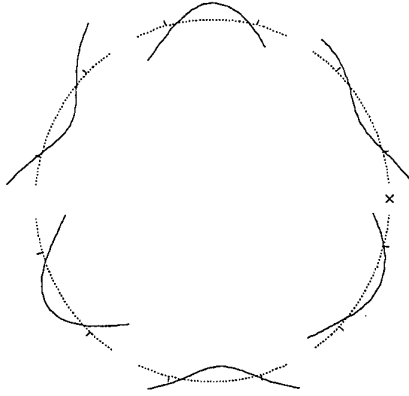
Mode Frequency: 1772 Hz



Mode Frequency: 1928 Hz



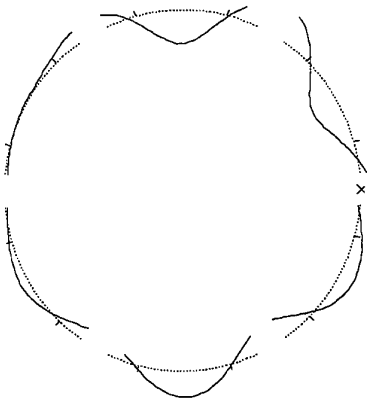
Mode Frequency: 2040 Hz



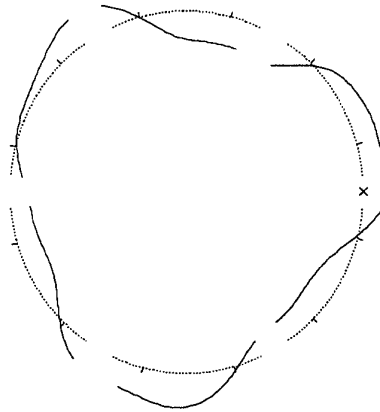


## Appendix B: Diagrams of mode shapes - interference

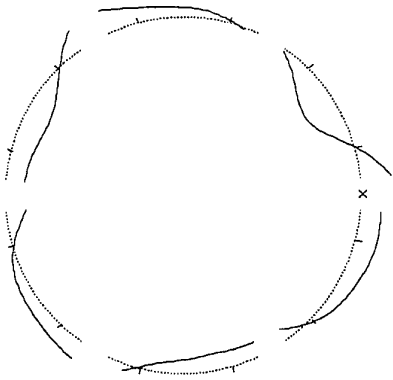
Mode Frequency: 1153 Hz



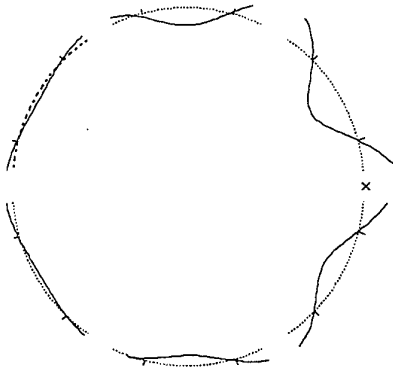
Mode Frequency: 1222 Hz



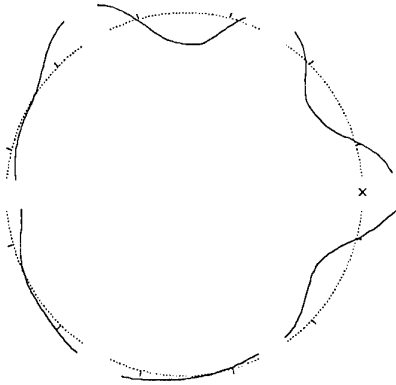
Mode Frequency: 1243 Hz



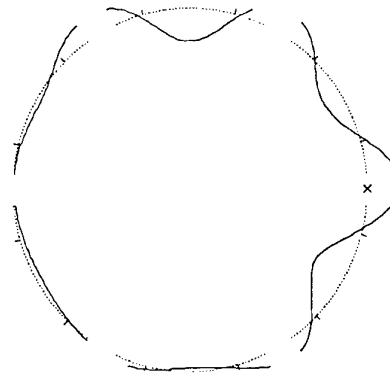
Mode Frequency: 1306 Hz



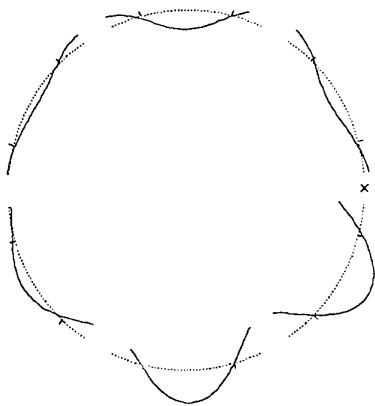
Mode Frequency: 1325 Hz



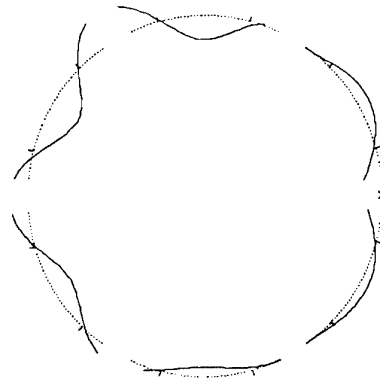
Mode Frequency: 1334 Hz



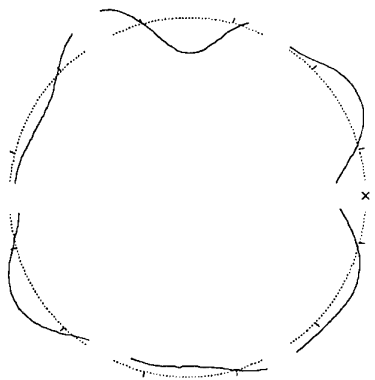
Mode Frequency: 1367 Hz



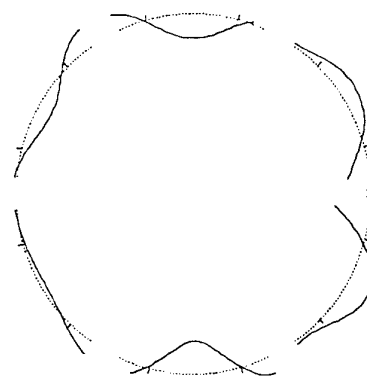
Mode Frequency: 1405 Hz



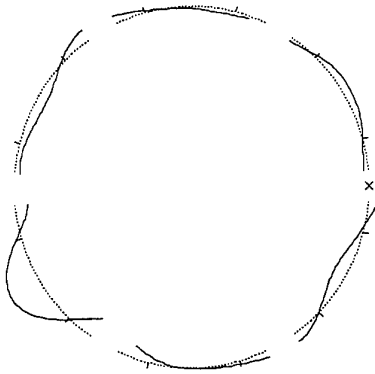
Mode Frequency: 1429 Hz



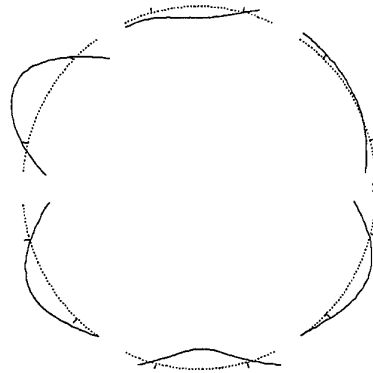
Mode Frequency: 1444 Hz



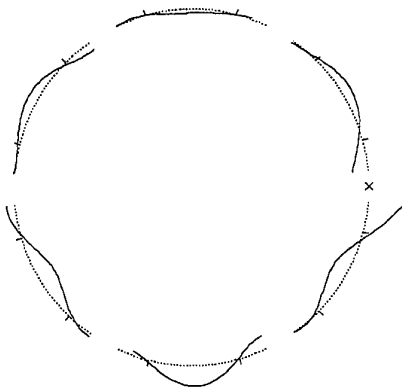
Mode Frequency: 1454 Hz



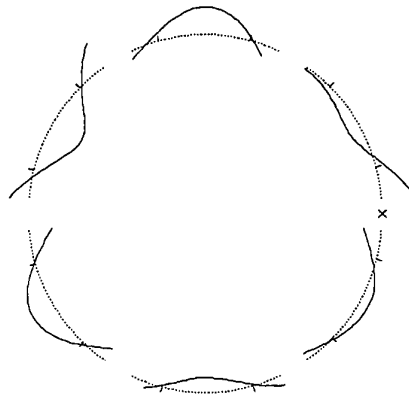
Mode Frequency: 1504 Hz



Mode Frequency: 1664 Hz



Mode Frequency: 1775 Hz



## DISTRIBUTION LIST

### Resonance Testing of the Gnome Combustor Liner

James Dunlop

#### AUSTRALIA

##### 1. DEFENCE ORGANISATION

###### a. Task Sponsor NALO

###### b. S&T Program

Chief Defence Scientist  
FAS Science Policy  
AS Science Corporate Management  
Director General Science Policy Development  
Counsellor Defence Science, London (Doc Data Sheet )  
Counsellor Defence Science, Washington (Doc Data Sheet )  
Scientific Adviser to MRDC Thailand (Doc Data Sheet )  
Director General Scientific Advisers and Trials/Scientific Adviser Policy and  
Command (shared copy)  
Navy Scientific Adviser  
Scientific Adviser - Army (Doc Data Sheet and distribution list only)  
Air Force Scientific Adviser  
Director Trials

} shared copy

###### Aeronautical and Maritime Research Laboratory

Director

Chief of Airframes and Engines Division

RLP

A. Wong

G. Stocks

J. Dunlop (4 copies)

###### DSTO Library

Library Fishermens Bend

Library Maribyrnong

Library Salisbury (2 copies)

Australian Archives

Library, MOD, Pymont (Doc Data sheet only)

###### c. Capability Development Division

Director General Maritime Development

Director General Land Development (Doc Data Sheet only)

Director General C3I Development (Doc Data Sheet only)

- d. **Navy**  
SO (Science), Director of Naval Warfare, Maritime Headquarters Annex, Garden Island, NSW 2000. (Doc Data Sheet only)
- e. **Army**  
ABCA Office, G-1-34, Russell Offices, Canberra (4 copies)
- g. **Intelligence Program**  
Defence Intelligence Organisation  
Library, Defence Signals Directorate (Doc Data Sheet only)
- i. **Corporate Support Program (libraries)**  
OIC TRS, Defence Regional Library, Canberra  
Officer in Charge, Document Exchange Centre (DEC), 1 copy  
\*US Defence Technical Information Centre, 2 copies  
\*UK Defence Research Information Center, 2 copies  
\*Canada Defence Scientific Information Service, 1 copy  
\*NZ Defence Information Centre, 1 copy  
National Library of Australia, 1 copy

## 2. UNIVERSITIES AND COLLEGES

Australian Defence Force Academy  
Library  
Head of Aerospace and Mechanical Engineering  
Senior Librarian, Hargrave Library, Monash University  
Librarian, Flinders University

## 3. OTHER ORGANISATIONS

NASA (Canberra)  
AGPS

## OUTSIDE AUSTRALIA

### 4. ABSTRACTING AND INFORMATION ORGANISATIONS

INSPEC: Acquisitions Section Institution of Electrical Engineers  
Library, Chemical Abstracts Reference Service  
Engineering Societies Library, US  
Materials Information, Cambridge Scientific Abstracts, US  
Documents Librarian, The Center for Research Libraries, US

### 5. INFORMATION EXCHANGE AGREEMENT PARTNERS

Acquisitions Unit, Science Reference and Information Service, UK  
Library - Exchange Desk, National Institute of Standards and Technology, US

SPARES (10 copies)

**Total number of copies: 59**

<b>DEFENCE SCIENCE AND TECHNOLOGY ORGANISATION DOCUMENT CONTROL DATA</b>				1. PRIVACY MARKING/CAVEAT (OF DOCUMENT)			
2. TITLE Resonance Testing of the Gnome Combustor Liner			3. SECURITY CLASSIFICATION (FOR UNCLASSIFIED REPORTS THAT ARE LIMITED RELEASE USE (L) NEXT TO DOCUMENT CLASSIFICATION)  Document (U) Title (U) Abstract (U)				
4. AUTHOR(S) James Dunlop			5. CORPORATE AUTHOR Aeronautical and Maritime Research Laboratory PO Box 4331 Melbourne Vic 3001				
6a. DSTO NUMBER DSTO-TN-0093		6b. AR NUMBER AR-010-266		6c. TYPE OF REPORT Technical Note		7. DOCUMENT DATE June 1997	
8. FILE NUMBER M1/9/317	9. TASK NUMBER NAV 95/270	10. TASK SPONSOR NALO		11. NO. OF PAGES 31		12. NO. OF REFERENCES 9	
13. DOWNGRADING/DELIMITING INSTRUCTIONS None			14. RELEASE AUTHORITY Chief, Airframes and Engines Division				
15. SECONDARY RELEASE STATEMENT OF THIS DOCUMENT  <i>Approved for public release</i>							
OVERSEAS ENQUIRIES OUTSIDE STATED LIMITATIONS SHOULD BE REFERRED THROUGH DOCUMENT EXCHANGE CENTRE, DIS NETWORK OFFICE, DEPT OF DEFENCE, CAMPBELL PARK OFFICES, CANBERRA ACT 2600							
16. DELIBERATE ANNOUNCEMENT No Limitations							
17. CASUAL ANNOUNCEMENT Yes							
18. DEFTEST DESCRIPTORS Gnome engines, combustors, vibration tests							
19. ABSTRACT This report details the results of a series of experimental tests conducted on a combustor liner of the Rolls-Royce Gnome engine. These tests were undertaken as part of an investigation into the cause of cracking of the combustor liner's splitter vane. A modal analysis of the splitter vane was undertaken and mode shape results are presented over a wide range of natural frequencies. A comparison of strains generated by these modes in the areas of cracking shows that two modes in particular are a possible cause of the cracking. The effects on the splitter vane, of an interference fit between it and the engine rear frame splitter ring, are also quantified both statically and dynamically.							

TECHNICAL NOTE DSTO-TN-0093 AR-010-266 JUNE 1997



AERONAUTICAL AND MARITIME RESEARCH LABORATORY  
GPO BOX 4331 MELBOURNE VICTORIA 3001  
AUSTRALIA, TELEPHONE (03) 9626 7000